Science of the Total Environment 616–617 (2018) 948–959

Contents lists available at ScienceDirect

Science of the Total Environment

journal homepage: www.elsevier.com/locate/scitotenv

A fast and easy approach to the simulation of binary mixtures sorption kinetics

L. Gusmaroli [a,d], C. Liu [b], J. Poch [c], N. Fiol [d,*], G. Alberti [a], I. Villaescusa [d]

[a] Dipartimento di Chimica, Università di Pavia, via Taramelli 12, 27100 Pavia, Italy
[b] College of Environmental Science and Engineering, Anhui Normal University, South Jiuhua Road 189, Wuhu 241002, Anhui, China
[c] Department of Applied Mathematics, Escola Politècnica Superior, Universitat de Girona, Avda. Maria Aurèlia Capmany, 61, 17003 Girona, Spain
[d] Chemical Engineering Department, Escola Politècnica Superior, Universitat de Girona, Avda. Maria Aurèlia Capmany, 61, 17003 Girona, Spain

HIGHLIGHTS

- Cr(VI) and Cu(II) sorption onto exhausted coffee encapsulated in gel beads
- Complex system: Sorption, redox reaction and ion exchange mechanism taking place
- Bench and pilot scale kinetics data modelling by Linear Adsorption Model (LAM)
- Development of an empirical model to quickly determine LAM parameters
- Simulation of process kinetics by combining LAM and the empirical model developed

GRAPHICAL ABSTRACT

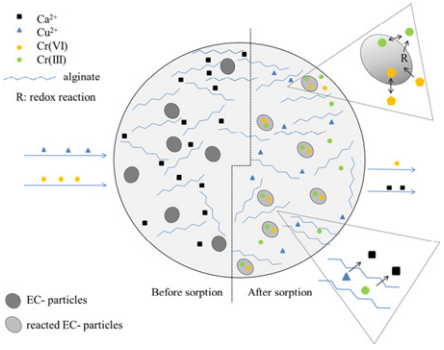

ARTICLE INFO

Article history:
Received 15 June 2017
Received in revised form 8 September 2017
Accepted 21 October 2017
Available online 6 November 2017

Editor: Henner Hollert

Keywords:
Biosorption
Modelling
Binary mixtures
Calcium alginate
Encapsulation
Divalent metals

ABSTRACT

Diffusivity of a component in a binary mixture is affected by the presence of a second component. The knowledge of the influence on each other component diffusivity is very useful for the prediction of sorption kinetics of binary mixtures. In this work kinetic studies of Cr(VI) and Cu(II) binary mixtures sorption onto exhausted coffee encapsulated in calcium alginate beads were carried out in both bench and pilot scale experiments. The spectroscopic analysis evidenced the complexity of the process since different mechanisms such as adsorption, redox reaction and ion exchange are involved. Experimental data were fitted to the Linear Adsorption Model (LAM). An empirical quadratic model was developed to estimate LAM parameters (D_e) and $\alpha = C_f/(C_i - C_f)$ as a function of the initial concentration of metals in the mixture. The empirical model developed enables to estimate the LAM parameters (D_e and α) of metal ions binary mixtures provided that the initial concentration of the metal ions is included in the range of concentrations studied. The estimated parameters introduced in LAM equation allow simulating the corresponding binary mixtures sorption kinetics. This study constitutes a fast and easy approach to the modelling of sorption kinetics of complex systems in which different processes take place simultaneously.

1. Introduction

Sorption processes in porous natural materials as a way to decontaminate wastewaters has attracted the attention of researchers during the last two decades. In our previous works exhausted coffee waste (EC)

* Corresponding author.
E-mail addresses: lgusmaroli@icra.cat (L. Gusmaroli), Jordi.poch@udg.edu (J. Poch), nuria.fiol@udg.edu (N. Fiol), Isabel.villaescusa@udg.edu (I. Villaescusa).

https://doi.org/10.1016/j.scitotenv.2017.10.225
0048-9697/

was investigated for Cr(VI) sorption in single and binary mixtures with Cu(II) (Fiol et al., 2008; Liu et al., 2015). In those works it was concluded that: Cr(VI) sorption by EC comprises reduction and sorption of Cr(VI) and Cr(III) and the presence of Cu(II) in the binary mixtures exerts a synergic effect on Cr(VI) sorption (Pujol et al., 2013). Exhausted coffee waste like most of bisorbents based on vegetable or agricultural wastes, is fragile and does not present either uniform or spherical shape. These characteristics make such materials unsuitable for large-scale processes. Encapsulation of biosorbents in polymeric matrixes such as calcium alginate has been used by some authors to solve the above mentioned problems. Calcium alginate has been successfully applied for the encapsulation of bacteria (Sag et al., 1995), algae (Aksu et al., 1998) and fungi (Bai and Abraham, 2003) for metal ions removal. More recently, agro food industry wastes such as grape stalks have been encapsulated for Cr(VI) sorption (Fiol et al., 2006; Sillerová et al., 2015; Escudero et al., 2017) while encapsulated sewage treatment plant waste metal (hydr)oxide was tested for arsenic removal (Escudero et al., 2009; Garlaschelli et al., 2017)). Calcium alginate beads themselves have proved to be efficient for divalent and trivalent metal ions removal by ion exchange between the calcium(II) in the beads and metal cations. (Chen et al., 1997; Ibañez and Umetsu, 2002; Cataldo et al., 2013; Escudero et al., 2017).

In this work, exhausted coffee has been encapsulated in calcium alginate beads to study Cr(VI) and Cu(II) adsorption kinetics in binary mixtures. It is well known that the kinetics of adsorption processes involve three consecutive steps: external diffusion of the solute through the liquid film that surrounds the solid particles, adsorption of the solute on the sorbent and internal diffusion across the particle by pore diffusion, surface diffusion or both of them. Depending on which is the rate-limiting step, different models are used to simulate the adsorption kinetics. The external-film diffusion model (Ponnusami et al., 2010; Sag and Aktay, 2000) describes the initial period of adsorption when the driving force is the concentration gradient located at the interface region between the bulk solution and the external surface of the adsorbent particles. The most used models when the adsorption step is considered to be the rate-limiting step are the pseudo-first order equation (Liu and Liu, 2008), pseudo-second order equation (Liu and Liu, 2008), Langmuir kinetic model (Placinski et al., 2009), Statistical Rate Theory (SRT) (Haerifar and Azizian, 2013; Placinski et al., 2009), and Elovich equation (Largitte and Pasquier, 2016). When intra-particle diffusion is the rate-limiting step the models used are the Weber-Morris equation or intraparticle model equation (Largitte and Pasquier, 2016; Liu and Liu, 2008; Sag and Aktay, 2000), the Fickian diffusion model (Ponnusami et al., 2010), the Film-pore diffusion model, the Linear Adsorption Model (LAM) (Chen et al., 1997; Papageorgiou et al., 2006), the Macropore and Micropore diffusion, the Macropore and Micropore parallel, the Shrinking Core Theory model, Homogeneous Surface Diffusion Model (HSDM) (Xu et al., 2013) and the Pore and Surface Diffusion model (Ma et al., 1996). In a multicomponent system as the studied in this work where several physical and chemical processes (sorption, reduction, ion exchange) take place the suitable model would be the Pore and Surface Diffusion model for a non-equilibrium multicomponent system. The use of this model requires estimating a set of unmeasured and hard-measuring parameters which makes the optimization process hard because of the large computational work required. Moreover, a specific experimental design is required to obtain the needed data to solve this complex mathematical problem.

Due to the complexity of the Pore and Surface Diffusion model and the large number of experiments required, the authors of the present study opted for testing simplified models with the least number of parameters that could explain the kinetics of the overall adsorption process of Cr(VI) and Cu(II) on exhausted coffee encapsulated in calcium alginate beads. Several models such as Weber-Morris and the Fickian Diffusion model were tested and the final choice was the Linear Adsorption Model that resulted to be the one that fitted best the experimental data. The advantage of this model is that only two parameters (D_e *and* α) for component of the mixture are needed. Furthermore, these parameters are of easy determination as $\alpha = C_f/(C_i - C_f)$ and D_e is obtained by solving a nonlinear equation. Once these two parameters were determined for each binary mixture, the foreseeable relationship between them and the initial concentration of the metals in the mixture was investigated by a regression model.

2. Experimental

2.1. Materials

Sodium alginate salt from brown algae purchased from Fluka was used as the hydrocolloidal gelling material. As fixing solution a $CaCl_2$ solution from Panreac (Barcelona, Spain) was used. Metal solutions were prepared by dissolving appropriate amounts of $K_2Cr_2O_7$ (Scharlau) and $CuCl_2 \cdot H_2O$ (Merk) in distilled water. NaOH and HCl 32% purchased from Panreac (Barcelona, Spain) were used for pH adjustment. Metal standard solution of 1000 mg/L purchased from Carlo Erba (Milano, Italy) was used for Atomic Absorption calibration.

Exhausted coffee (EC) waste was kindly provided by a soluble coffee production plant from Catalonia region (Spain). The waste was first oven dried at 105 °C until constant weight and then ground and sieved to obtain a particle size of 50–100 μm.

2.2. Preparation of the beads

The beads were prepared according to the procedure followed by Fiol et al. (2005). A 1% (w/v) Na-alginate solution was prepared by solving 1 g of sodium alginate into 100 mL distilled water at a temperature of about 65 °C. Then, the gel was allowed to cool down at room temperature and 2 g of exhausted coffee powder (50–100 μm) was added to the gel with continuous stirring. Once the mixture was homogeneous it was forced through a micropipette tip by a peristaltic pump. The resulting gel droplets were collected in a stirred reservoir containing 200 mL of a chemical "fixing" solution of 0,1 M $CaCl_2$. The beads were allowed to harden in this solution for 24 h. After this time hard spherical beads containing 2% (w/v) of exhausted coffee were obtained. The microbeads were filtered and rinsed several times with distilled water to remove calcium chloride from the bead surface. Then they were stored in distilled water at 4 °C until their use. When calcium alginate beads were used as a blank, the same procedure was followed but in this case there was no addition of exhausted coffee powder. The average diameter of the obtained beads determined by optical microscopy was 3.14 ± 0.14 mm. Once produced the beads were stored in Milli-Q water at 4 °C. The different beads will be referred to as CA (calcium alginate beads) and EC-CA (calcium alginate beads containing exhausted coffee).

2.3. Beads physical characterization

CA and EC-CA beads properties that are likely to be related to their sorption performance namely water content, weight swelling ratio, diameter and density were determined. Morphological and elemental analysis of the beads by Scanning Electron Microscopy (SEM) coupled with Energy Dispersive X-Ray Spectroscopy (EDX) was also carried out. The presence of reduced species of chromium sorbed onto the beads was examined by ESR (Electron Spin Resonance).

2.3.1. Water content and weight swelling ratio (WSR)

The dry weight of 40 beads was determined drying the beads at 40 °C until constant weight was reached. To measure the wet weight the same amount of beads were placed onto a cellulose filter paper

for 1 min and then weighted immediately. The average of five dry and wet weight determinations as well as the standard deviations was determined. The weight swelling ratio (WSR) was estimated as the ratio of wet and dried beads weights.

2.3.2. Beads diameter and density

The diameter of 40 beads was measured by using a Vernier caliper. Mean value and the corresponding standard deviation were calculated.

Beads density mass of the beads was determined by putting 5 mL of milli-Q water in a 10 mL cylinder placed on a balance and adding 40 beads. The mass of beads was determined by difference between the mass of cylinder without and with the beads. The volume of the beads by reading the increase of volume in the graduated cylinder marks as a consequence of beads addition to the Milli-Q water.

2.3.3. SEM/EDX analysis

The beads morphology was analysed by SEM (Zeiss-DSM Scanning Electron Microscope). Elemental analysis was performed by using an X-ray Energy Dispersive (EDX) detector coupled with the microscope. Before the analysis the samples were dried at 105 °C and their surface coated with gold in the presence of argon by an Edwards Sputter Coater S150A in order to prevent charging under electronic beam.

2.3.4. ESR analysis

Cr(III) having unpaired electrons provides a positive ESR signal. For this analysis 40 beads of EC-CA were put into contact with a 100 mg/L Cr(VI) solution (pH 3.0) for 48 h under agitation. As water strongly absorbs microwave energy, samples were dried in an oven for about 24 h, crushed and loaded in a quartz sample tube. The analysis was performed at room temperature using an ESR Spectrometer Bruker ELEXSYS E580 (microwave frequency Q-band = 34.082 GHz, modulation frequency = 100 kHz, modulation amplitude = 3 G, central field = 12,000 G, field sweep = 4000 G, power = 1.968 mW, power attenuation = 20 dB).

2.4. Sorption studies

Previous studies reported pH = 3.0 as a suitable pH for Cr(VI) and binary mixtures of Cr(VI) and Cu(II) sorption onto EC (Fiol et al., 2008; Pujol et al., 2013; Liu et al., 2015). Therefore all prepared metal ions solutions were adjusted at pH 3.0 by adding 1.0 M HCl drops. In order to investigate the influence of the presence of Cu(II) on Cr(VI) sorption by 2% EC-CA beads, binary mixtures of Cr(VI) and Cu(II) at different concentration ratio were prepared. Table 1 shows the composition of single metal ion and binary mixtures solutions used in bench and pilot scale experiments.

2.4.1. Bench scale experiments

Sorption studies were performed by putting into contact 40 EC-CA beads with 15 mL of Cr(VI) and Cu(II) binary mixtures solutions in stoppered glass tubes. The tubes were shaken in a rotary stirrer (Rotator drive STR 4, Stuart Scientific) until equilibrium was attained. To ensure constant temperature throughout the whole process, the stirrer was placed inside an incubator (Memmert) where the temperature was set at 20 °C. All experiments were performed in duplicate and the average value is presented.

Table 1
Metals initial concentration in mM of binary mixtures used for bench and pilot scale.

		Bench scale				Pilot scale		
		Cu(II)				Cu(II)		
		0	0,2	0,4	0,6	0,2	0,4	0,6
Cr(VI)	0,2						x	x
	0,4	x	x	x	x	x	x	x
	0,6	x	x	x	x	x	x	
	0,8	x	x	x	x			

Table 2
Beads physical properties.

Properties	CA beads	EC-CA beads
Weight of 40 wet beads (g)	0,850 ± 0,004	0,859 ± 0,006
Weight of 40 dry beads (g)	0,0163 ± 0,0006	0,0487 ± 0,0006
Water content (%)	98,1 ± 0,2	94,3 ± 0,1
Weight swelling ratio (WSR)	52,0 ± 0,4	17,6 ± 0,3
Diameter (cm)	0,32 ± 0,01	0,34 ± 0,01
Density (g mL^{-1})	1,01 ± 0,01	1,23 ± 0,02

2.4.2. Pilot scale experiments

Experiments were performed in a 5 L stirred reactor under continuous agitation (350 rpm) at room temperature (20 ± 2 °C). The reactor is closed by a detachable glass cap with different openings that enable the introduction of the sorbent, the paddle agitator and the sampling tube. For all the experiments a volume of 4 L of metal ions binary mixtures solution was contacted with 2500 beads for 5 days. All experiments were performed in duplicate and the average value is presented.

2.4.3. Metal ions analysis

After the sorption process, the sorbent was removed by filtration and pH of the remaining solution was measured using a Crison Model Digilab 517pH meter.

The initial and final copper and total chromium concentration in the filtrates, were determined by Flame Atomic Absorption Spectrometry (FAAS) (Varian Absorption Spectrometer SpectrAA 220FS). In order to determine whether chromium was exclusively present in the hexavalent oxidation state or also as Cr (III), Cr(VI) concentration was determined by the standard colorimetric 1,5-diphenylcarbazide method by using a sequential injection system (SIA) recently developed in our laboratory. The concentration of Cr(III) was determined as the difference between total chromium and hexavalent chromium concentration. The Cr(VI) standard used for obtaining the calibration curves in the diphenylcarbazide method was analysed by FAAS. Analytical measurements made by the two techniques comparable within 5%. Before analysis, samples were acidified by adding 1 M HCl to avoid possible precipitation of divalent metal ions.

2.5. Kinetics modelling

The model used in this work for the quantitative description of the overall sorption dynamics of the studied process assumes: (i) the liquid-film mass transfer is eliminated by stirring, (ii) the limiting rate is intraparticle diffusion, (iii) the beads are homogeneous spheres (Papageorgiou et al., 2006; Ponnusami et al., 2010) and (iv) local equilibrium between ions in solid and liquid phase is expressed as $q = KC$ (Crank, 1975). With these hypotheses the mass balance in the intraparticle pore diffusion is expressed as:

$$\frac{\partial C}{\partial t} = D\left(\frac{1}{r^2}\,\frac{\partial}{\partial r}\left(r^2\frac{\partial C}{\partial r}\right)\right) \quad (1)$$

where $D = \dfrac{D_e}{1 + \dfrac{1-\varepsilon_p}{\varepsilon_p}\rho K}$

And the mass balance in the liquid phase is expressed as:

$$-V\frac{dC_L}{dt} = M\frac{d\overline{q}}{dt} \quad (2)$$

where

$$\overline{q} = \frac{3}{R^3}\int_0^R q\, r^2\, dr \quad (3)$$

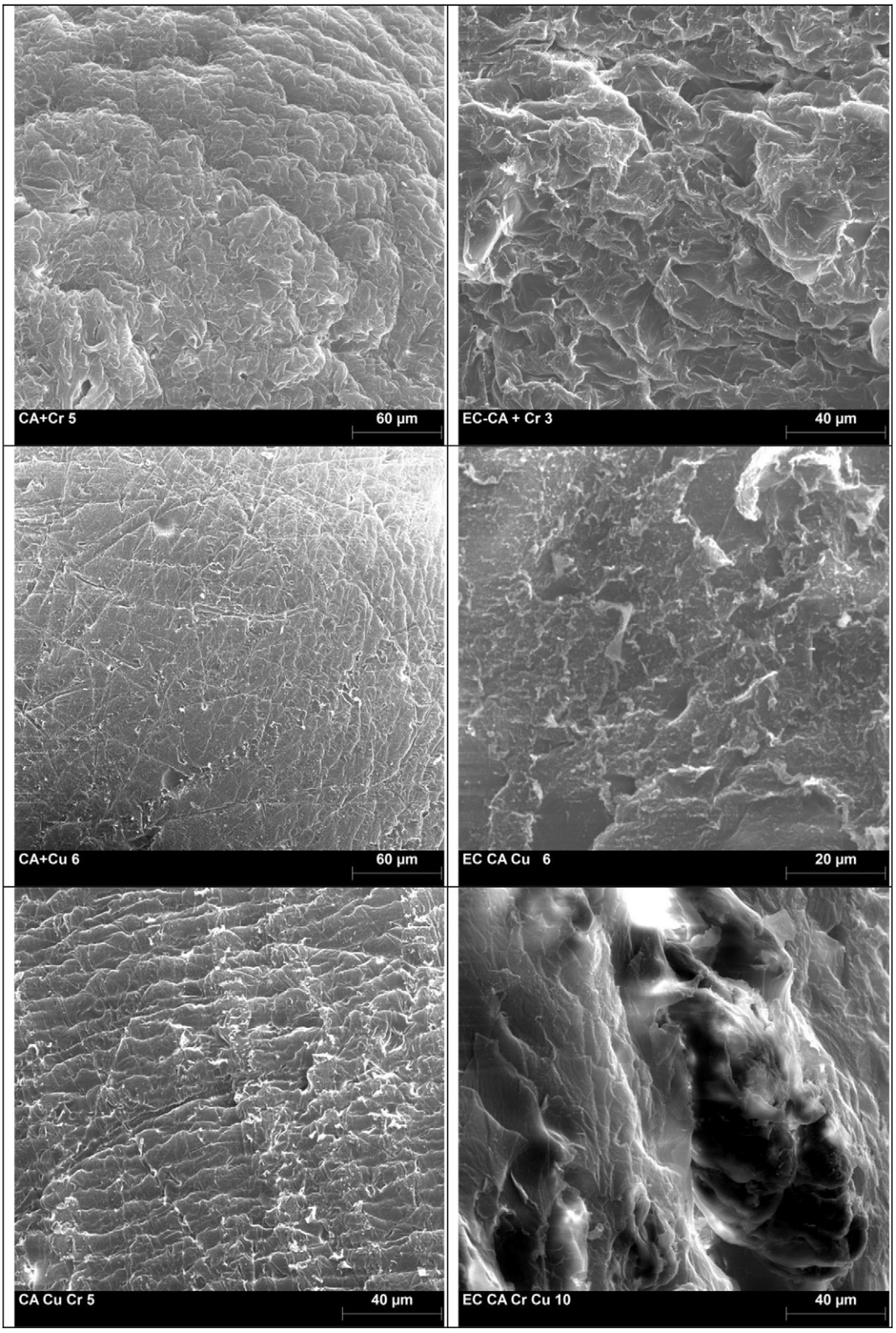

Fig. 1. Beads SEM micrographs (a) CA loaded with Cr(VI) (b) EC-CA loaded with Cr(VI) (c) CA loaded with Cu(II) (d) EC-CA loaded with Cu(II) (e) CA loaded with Cr(VI) and Cu(II) and (f) EC-CA loaded with Cr(VI) and Cu(II).

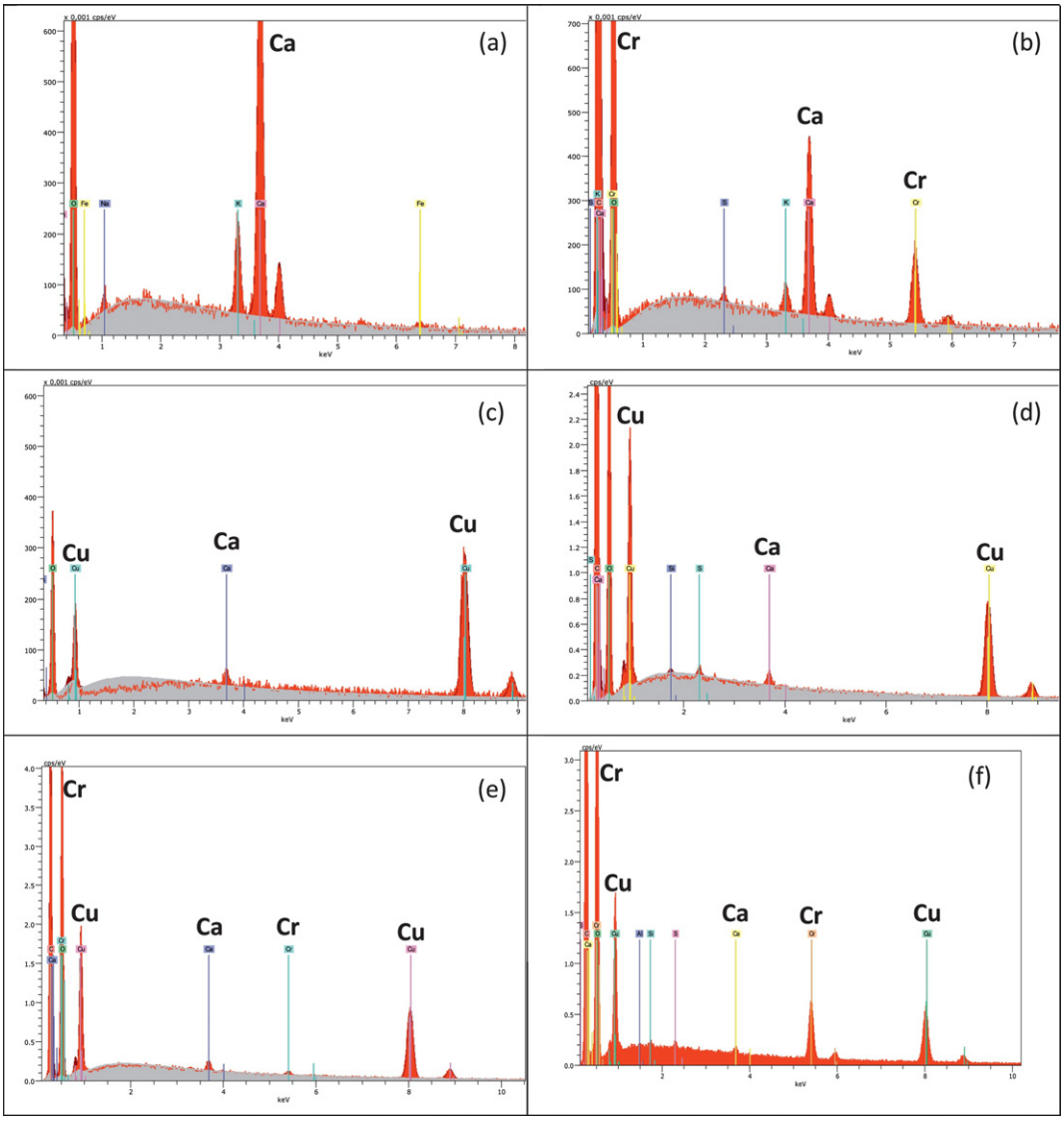

Fig. 2. Beads EDX spectra (a) CA loaded with Cr(VI) (b) EC–CA loaded with Cr(VI) (c) CA loaded with Cu(II) (d) EC-CA loaded with Cu(II) (e) CA loaded with Cr(VI) and Cu(II) and (f) EC-CA loaded with Cr(VI) and Cu(II).

Substituting Eq. (3) in Eq. (2), taking into account that $\rho q = C$ and the intraparticle pore diffusion (Eq. 1), Eq. (2) can be written as:

$$-V\frac{dC_L}{dt} = \rho V_p \frac{3}{R^3}\int_0^R \frac{\partial q}{\partial t} r^2 dr = V_p \frac{3}{R^3}\int_0^R \frac{\partial C}{\partial t} r^2 dr$$
$$= V_p \frac{3D}{R^3}\int_0^R \frac{\partial}{\partial r}\left(r^2 \frac{\partial C}{\partial r}\right) dr$$

and calculating the integral:

$$V\frac{dC_L}{dt} = -D\, 4\pi R^2 N \left(\frac{\partial C}{\partial r}\right)_{r=R} \quad (4)$$

with the initial conditions:

$$C_L = C_0 \quad t = 0$$

$$C = C_0 \quad t = 0, r = R$$

$$C = 0 \quad t = 0, r < R \quad (5)$$

and boundary conditions for Eq. (1):

$$C = C_L \quad t > 0, r = R$$

$$\frac{\partial C}{\partial r} = 0 \quad t > 0, r = 0 \quad (6)$$

where C is the concentration of metal in the liquid phase inside the beads, q the amount of metal in the solid phase inside the beads, C_L the concentration of metal in the solution, C_0 the initial concentration of metal in the liquid phase, R the radius of the beads, N the number of beads, ε_p the porosity of the beads, V the volume of the solution and D_e the diffusion coefficient.

The analytical solution of Eq. (1) with the initial conditions Eq. (5) and the boundary conditions Eq. (6) is:

$$C(t,r) = \frac{\alpha C_0}{1+\alpha}\left[1 + 6(1+\alpha)\sum_{n=1}^{\infty} \frac{e^{-\frac{D S_n^2}{R^2}t}}{9 + 9\alpha + \alpha^2 S_n^2} \frac{R}{r} \frac{\sin\left(S_n \frac{r}{R}\right)}{\sin(S_n)}\right] \quad (7)$$

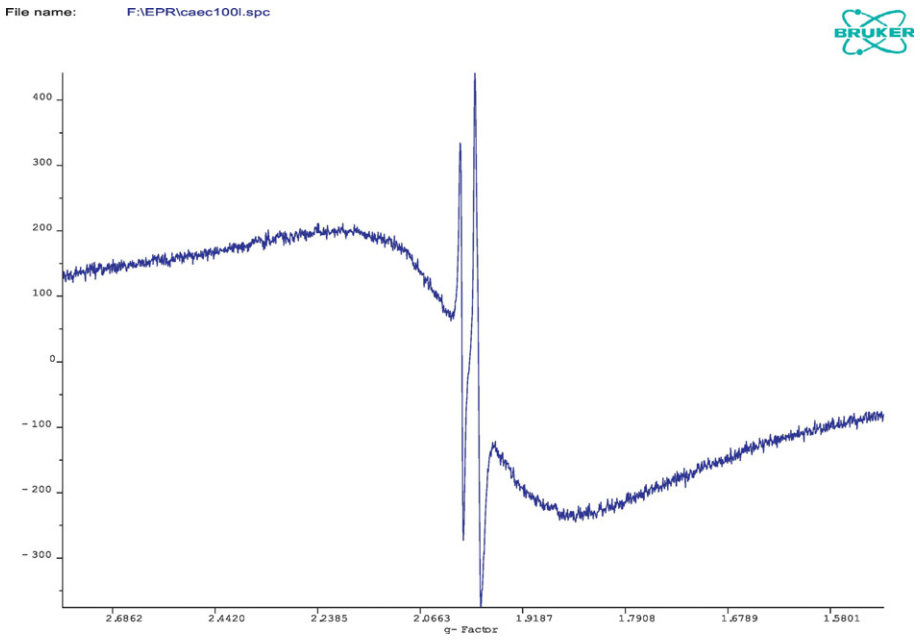

Fig. 3. ESR spectrum of Cr(VI)-laden EC–CA beads.

where $\alpha = \frac{C_\infty}{C_0 - C_\infty}$ and S_n are the solutions of Eq. (8)

$$1 - \frac{S_n}{tan(S_n)} = -\frac{\alpha}{3} S_n^2 \tag{8}$$

Eq. (8) has infinite solutions from which we used 200 to get an approximation of $C(t,r)$ of Eq. (7).

The effective diffusion coefficient D_e was determined by least square method of the analytical solution Eq. (7) of each of the experimental data set (bench and pilot plant scale) by minimising the Sum Squares Residual Eq. (9):

$$SSR = \sum_{i=1}^{M} (C_i - C(t_i, R, D))^2 \tag{9}$$

Minimisation of SSR is as simplest as solving Eq. (10) by using the method of Newton- Raphson.

$$\frac{\partial SSR}{\partial D} = \sum_{i=1}^{m} \left[2(C(t_i) - C(t_i, D)) \left(-\frac{\partial C(t_i, D)}{\partial D} \right) \right] = 0 \tag{10}$$

In general, all the calculations were made by using Matlab R2015a.

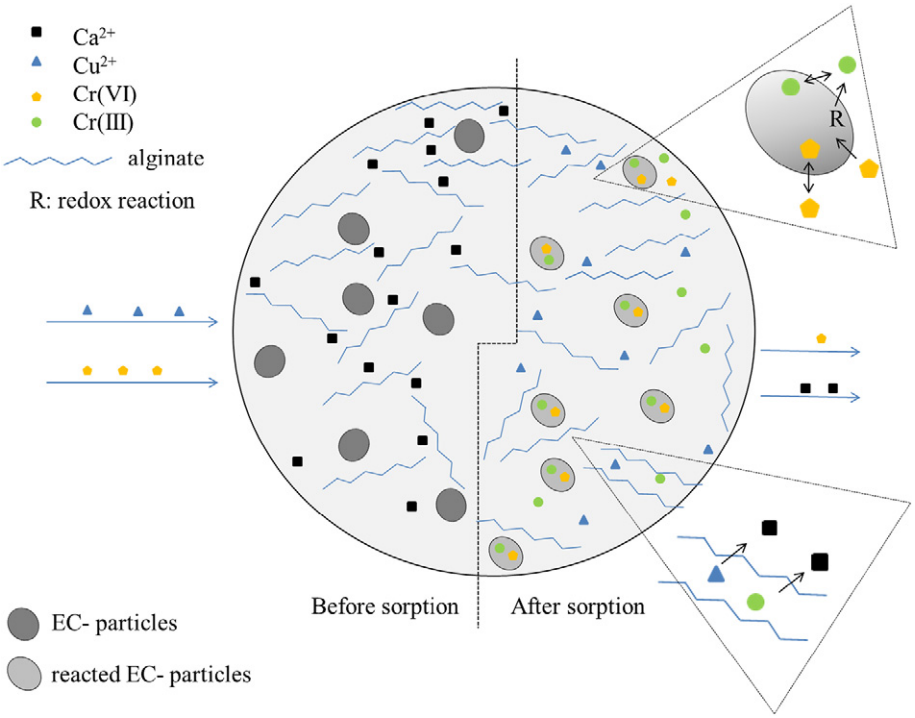

Fig. 4. Schematic representation of the processes contributing to Cr(VI and Cu(II) sorption onto EC–CA beads.

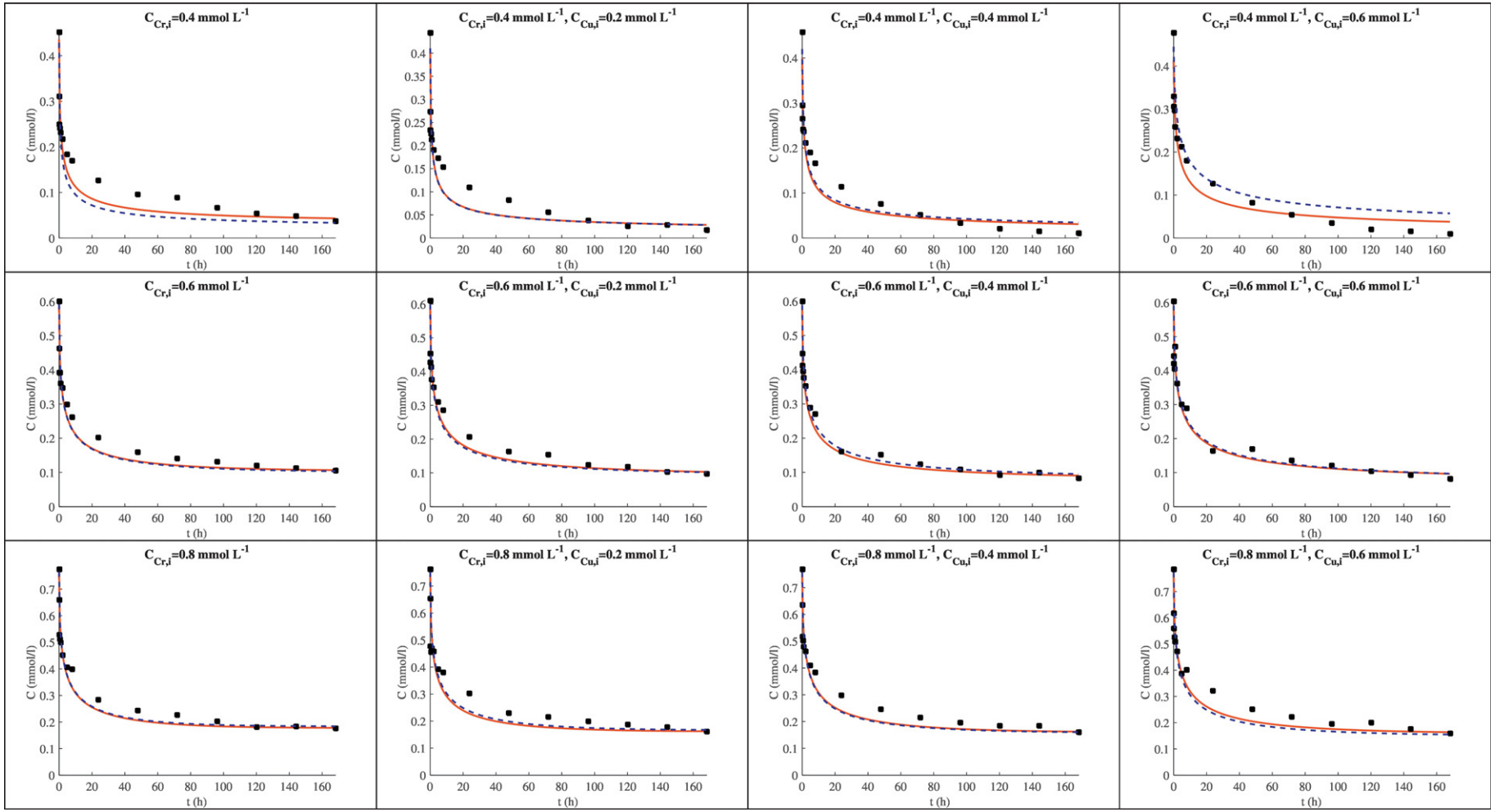

Fig. 5. Chromium sorption kinetics of bench studies. Experimental data points, LAM model simulation (solid line) and empirical simulation (dashed line).

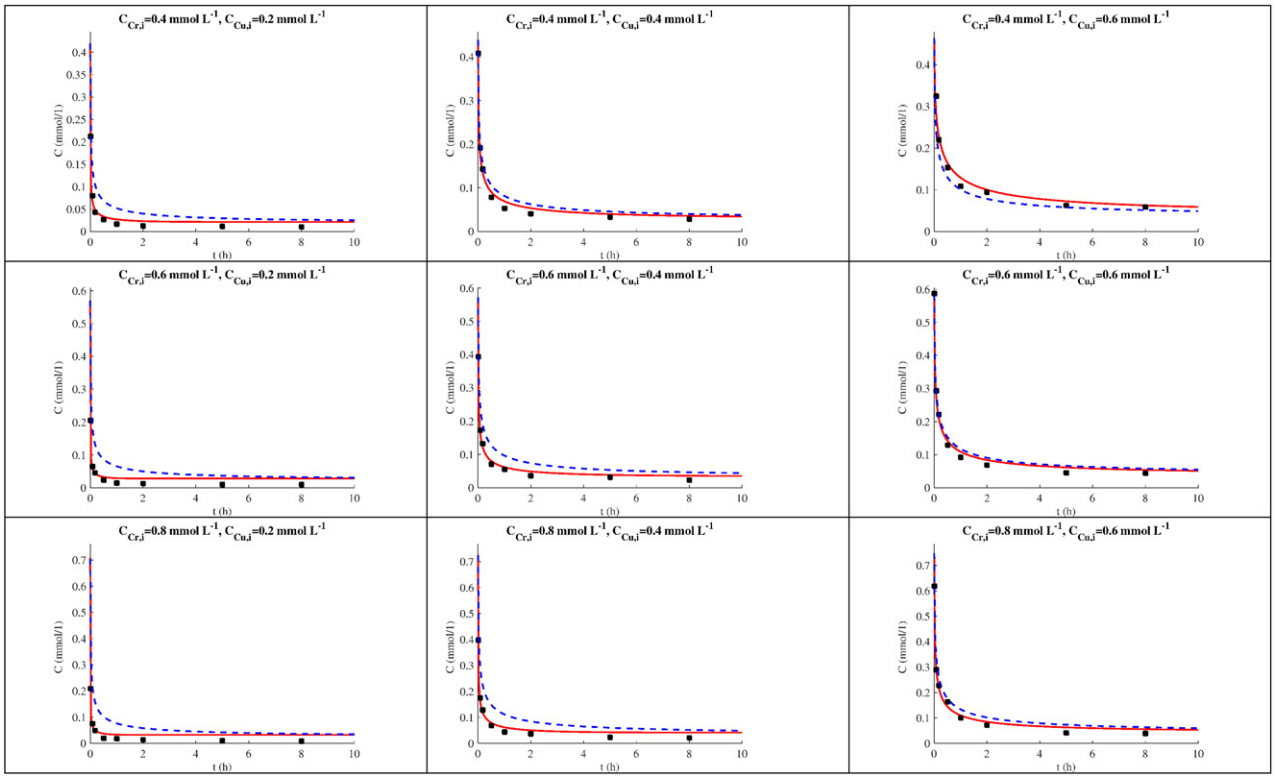

Fig. 6. Copper sorption kinetics of bench studies. Experimental data points, LAM model simulation (solid line) and empirical simulation (dashed line).

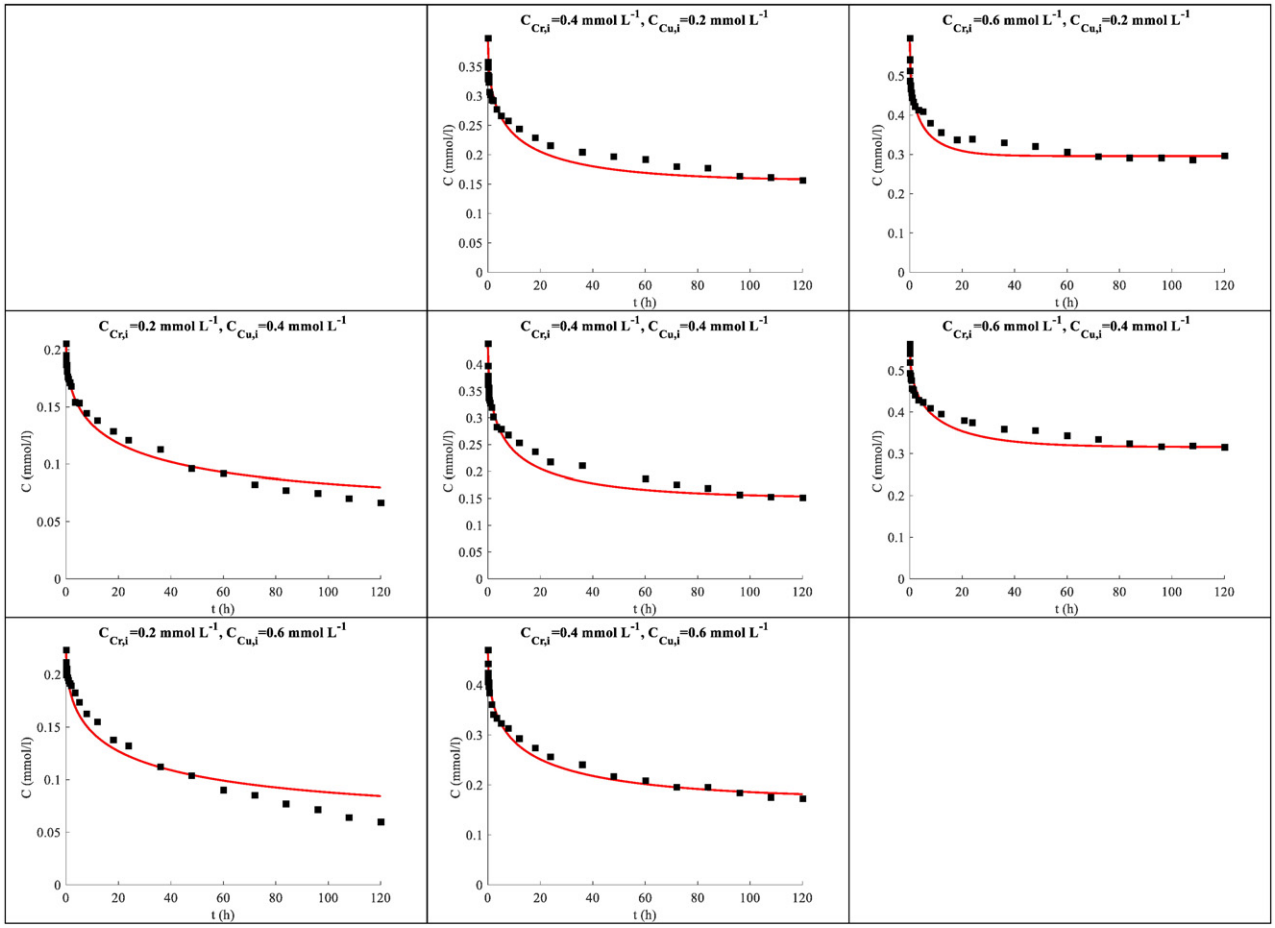

Fig. 7. Chromium sorption kinetics of pilot plant studies. Experimental data points and LAM model simulation (solid line).

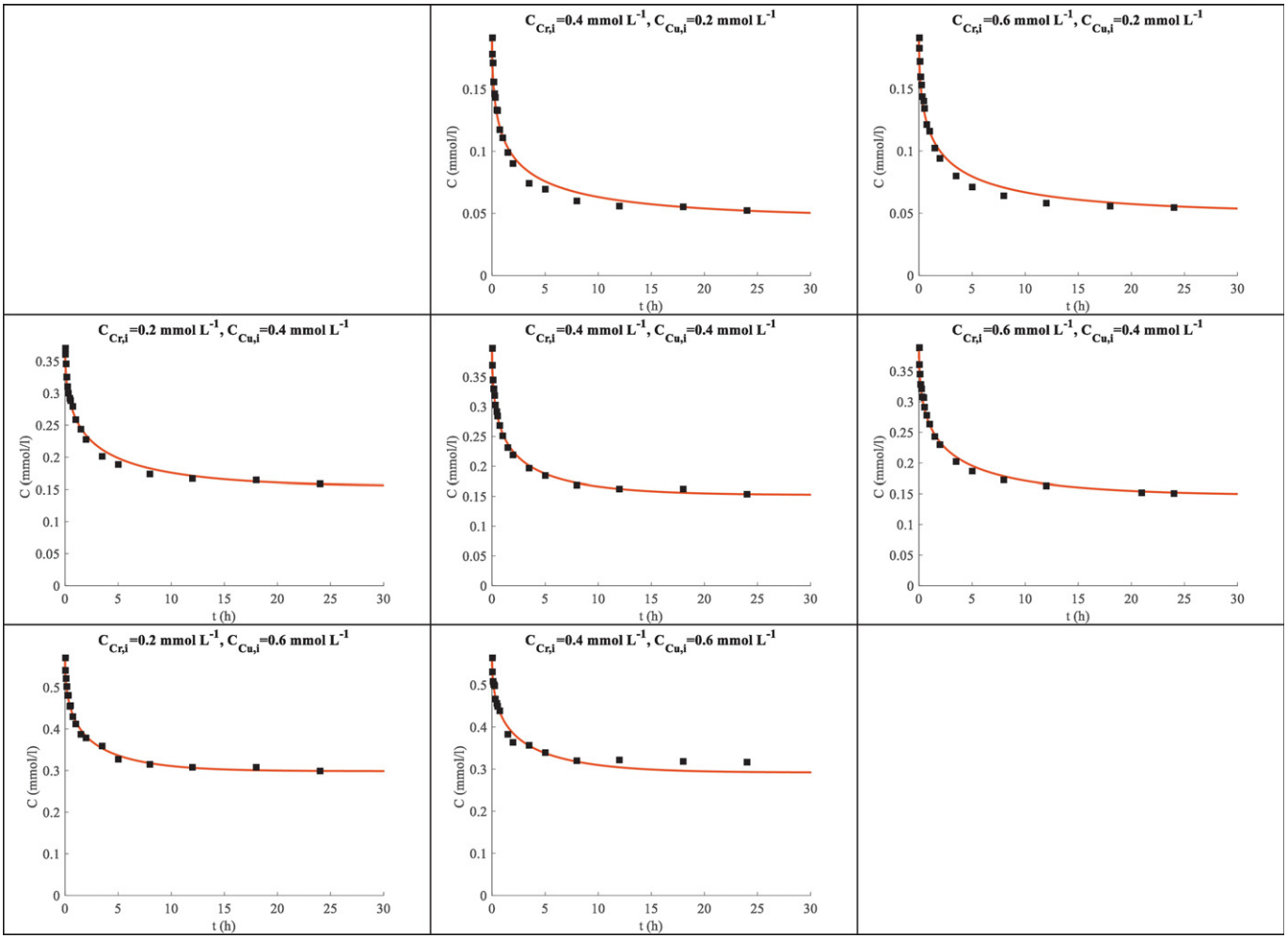

Fig. 8. Copper sorption kinetics of pilot plant studies. Experimental data points and LAM model simulation (solid line).

3. Results and discussion

3.1. Beads characterisation

The results of beads physical characterisation are shown in Table 2. As seen in the table weight and diameter of wet beads are similar while a slightly greater weight and larger mean diameter are observed for EC-CA beads. Compared to CA, EC-CA beads show greater weight of dry beads and density and lower water content, and WSR. Similar trends in beads characteristics were found by other authors that encapsulated biomass in calcium alginate (Fiol et al., 2005; Sillerová et al., 2015).

Micrographs from Scanning Electron Microscopy (SEM) analysis of the beads show wrinkled surfaces with pores and creases, especially

Table 3
Model parameters for Cr(VI) and Cu(II) sorption obtained by fitting bench scale sorption data. *D* units (cm^2/h).

	D Cr(VI)				*D* Cu(II)			
	Cu (mM)				Cu (mM)			
	0	0,2	0,4	0,6	0	0,2	0,4	0,6
Cr (mM)								
0,4	2,66E-03	1,67E-03	7,30E-04	4,59E-04		9,27E-02	5,62E-02	5,53E-02
0,6	2,84E-03	2,03E-03	2,04E-03	1,41E-03		1,12E-01	5,25E-02	4,84E-02
0,8	2,89E-03	2,93E-03	2,42E-03	2,20E-03		8,10E-02	5,35E-02	3,99E-02
	α Cr(VI)				α Cu(II)			
	Cu (mM)				Cu (mM)			
	0	0,2	0,4	0,6	0	0,2	0,4	0,6
Cr (mM)								
0,4	8,98E-02	3,87E-02	2,40E-02	2,21E-02		5,07E-02	7,47E-02	1,08E-01
0,6	2,11E-01	1,88E-01	1,59E-01	1,54E-01		4,84E-02	6,15E-02	7,96E-02
0,8	2,97E-01	2,69E-01	2,62E-01	2,56E-01		4,45E-02	5,73E-02	6,60E-02

Table 4
Model parameters for Cr(VI) and Cu(II) sorption obtained by fitting pilot plant sorption data. *D* units (cm^2/h).

	D Cr(VI)			*D* Cu(II)		
	Cu (mM)			Cu (mM)		
	0,2	0,4	0,6	0,2	0,4	0,6
Cr (mM)						
0,2		2,52E-03	2,35E-03		3,12E-02	3,63E-02
0,4	6,73E-03	7,68E-03	4,74E-03	3,88E-02	4,68E-02	3,81E-02
0,6	1,77E-02	6,91E-03		3,41E-02	3,42E-02	
	α Cr(VI)			α Cu(II)		
	Cu (mM)			Cu (mM)		
	0,2	0,4	0,6	0,2	0,4	0,6
Cr (mM)						
0,2		4,76E-01	4,32E-01		8,20E-01	1,18E + 00
0,4	6,43E-01	5,28E-01	5,81E-01	4,14E-01	6,90E-01	1,30E + 00
0,6	9,83E-01	1,27E + 00		4,36E-01	7,21E-01	

when beads are loaded with chromium (Fig. 1). EDX spectra of Fig. 2 clearly show the poor sorption of chromium onto CA beads (Fig. 2(a and e)) and the decrease of calcium when CA beads are copper-laden (Fig. 2 (c and e)). This last observation confirms that copper(II) is sorbed via ion exchange with calcium(II) ions of the gel. The role of exhausted coffee in chromium sorption is evident in Fig. 2 (b and f). Chromium appears in these two spectra proving chromium sorption. The decrease of calcium(II) ions in Fig. 2 (b) cannot be quantitatively related to chromium sorption due to the semi-quantitative character of EDX analysis. Nevertheless taking into account that Cr(VI) is reduced to Cr(III) by the action of EC (Liu et al., 2016) a decrease in calcium(II) ions is expected. Therefore the decrease of calcium(II) might be attributed to the exchange of this cation with newly formed trivalent chromium. Accepting that Cr(III) exchanges with calcium(II), the important decrease of calcium(II) observed in Fig. 2 (f) could be due to the exchange of this cation with both trivalent chromium and copper(II) ions as EC-CA beads were loaded with both Cr(VI) and Cu(II). No clear differences between copper-laden CA and EC-CA beads spectra (Fig. 2 (c and d) could be stablished. This result was expected as the main responsible of copper(II) sorption is calcium alginate while copper(II) sorption onto EC is negligible, due to the small amount of EC in EC-CA beads. The lower sorption of EC for copper compared to chromium was reported in Pujol et al., 2013.

The ESR spectrum of CA chromium(VI) loaded beads produced a very weak signal (not shown here) which indicates the low capacity of calcium alginate to reduce Cr(VI). Conversely, ESR spectrum of EC-CA beads loaded with Cr(VI) showed the intense signals relative to reduced species of chromium (Fig.3). The three unpaired electrons of Cr(III) produce the wave-like signal that is observed in the whole range (2.82–1.54 g-factor). A small and sharp peak in the middle (1.993 g-factor) corresponds to Cr(V) that is ESR-sensitive because it has an unpaired electron. Analogous spectra were also obtained for grape stalk encapsulated in calcium alginate beads (Escudero et al., 2006), coir pit (Suksabye et al., 2009) and wood (Humar et al., 2004). The results presented in Fig. 3 prove that EC particles are responsible for Cr(VI) reduction and the formation of trivalent and to a lesser extent pentavalent species of chromium.

From SEM and ESR analyses of metal-laden CA and EC-CA beads the different processes that take place in the simultaneous sorption of Cr(VI) and Cu(II) onto EC-CA beads are summarised and graphically depicted in Fig. 4. The figure aims to describe the processes undergone by the components of both the sorbent (CA and EC) and the metal solution (Cr(VI) and Cu(II)) on the basis of the above described mechanisms that take place: redox reaction, sorption, and ion exchange.

3.2. Sorption studies

The experimental kinetics data of Cr(VI) and Cu(II) obtained from bench studies are plotted in Figs. 5 and 6, respectively. As observed, kinetics of Cr(VI) is much slower than Cu(II) kinetics. After two hours copper(II) sorption is more than 90% of maximum sorption and the 100% is achieved at around 5 h in all the binary mixtures. In the case of chromium, equilibrium is reached after 120 h and the maximum percentage of sorption is within the range 77–97% that corresponds to the highest concentration of chromium sorbed in the absence of copper(II) or the lowest concentration of chromium sorbed at the highest copper(II), respectively. These results are in accordance with the reported synergistic effect on Cr(VI) and Cu(II) sorption when using EC (Pujol et al., 2013).

The plot of the kinetics data from pilot plant studies are plotted in Figs. 7 and 8 for Cr(VI) and Cu(II) respectively. As shown in the figures sorption kinetics are lower than the ones found for bench studies. After 120 h chromium did not reach equilibrium in any of the tested binary mixtures and around 24 h were necessary for copper sorption equilibrium. The sorption rates were also lower and did not exceed 75% in any case. The explanation for these worse results is that the ratio between the volume of binary mixture solution and the number of beads is enormously lower in the case of the reactor (23.5% of the ratio used in tubes experiments). The ratio used for bench studies was not suitable for the pilot plant due to operational conditions. The great number of beads needed to keep this ratio (10,667 beads) would require of a very high agitation speed to maintain the complete mixing that would provoke beads damaging.

The faster kinetics of copper compared to chromium kinetics is compatible with an ion exchange mechanism with calcium cations of the CA beads (Cataldo et al., 2013). This hypothesis was confirmed by EDX analyses.

It must be pointed out that the concentration of Cr(III) in the remaining solution of both bench and pilot plant sorption experiments was negligible (lower than FAAS detection limit for Cr). The almost absence of trivalent chromium in the final solutions indicates that the reduced

Table 5
Empirical model parameters (*D* and α) for Cr(VI) and Cu(II) sorption obtained by fitting bench sorption data. *D* units (cm^2/h).

	D Cr			
	Estimate	SE	tStat	pValue
k_1	2,781E-03	1,131E-04	24,589	1,46E-09
$k_{1,Cu}$	−9,425E-03	9,220E-04	−10,222	2,98E-06
$k_{1,Cr,Cu}$	1,126E-02	1,398E-03	8053	2,10E-05
R^2	0,935			
	α Cr			
	Estimate	SE	tStat	pValue
k_2	−2,751E-01	2,848E-02	−9661	4,76E-06
$k_{2,Cr}$	7,679E-01	4,776E-02	16,077	6,17E-08
$k_{2,Cr,Cu}$	−1,592E-01	4,163E-02	−3823	4,07E-03
R^2	0,966			
	D Cu			
	Estimate	SE	tStat	pValue
k_3	1,780E-01	2,699E-02	6597	5,83E-04
$k_{3,Cu}$	−4,923E-01	1,496E-01	−3291	1,66E-02
$k^2_{3,Cu}$	4,576E-01	1,821E-01	2514	4,57E-02
R^2	0,868			
	α Cu			
	Estimate	SE	tStat	pValue
k_4	2,637E-02	4,597E-03	5737	1,22E-03
$k_{4,Cu}$	2,131E-01	2,223E-02	9586	7,37E-05
$k_{4,Cr,Cu}$	−1,884E-01	3,067E-02	−6142	8,53E-04
R^2	0,950			

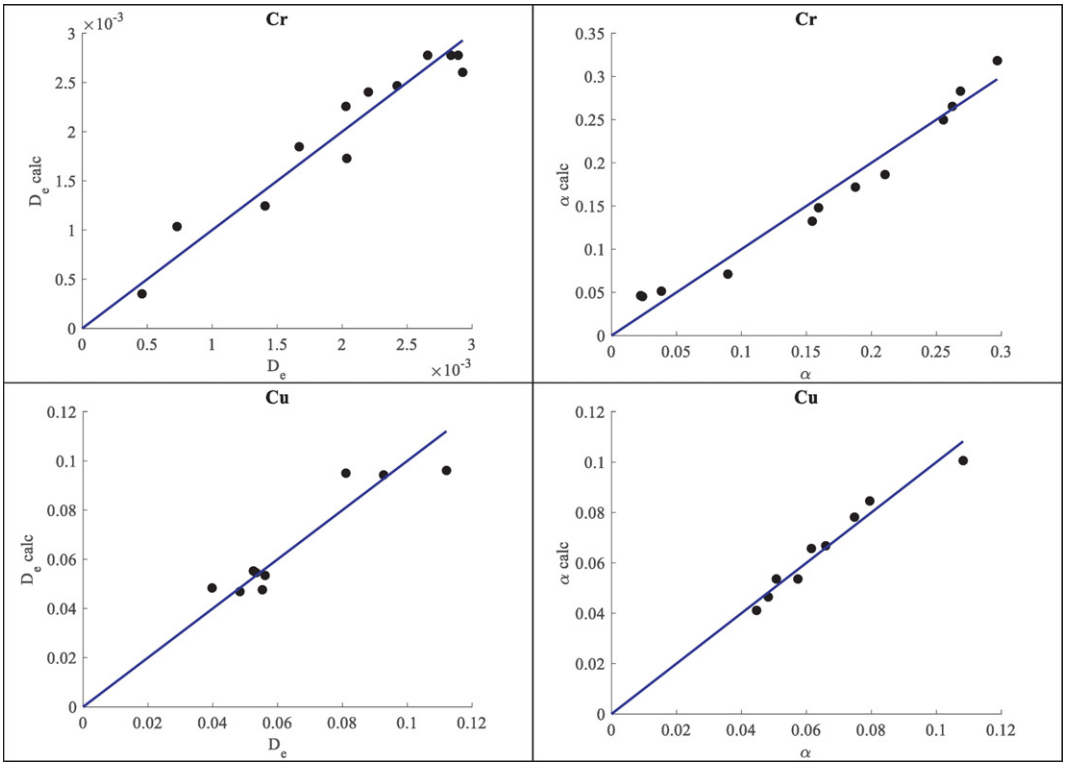

Fig. 9. Plot of D_e and α coefficients values calculated by the empirical model vs. coefficients obtained by the LAM model a) Cr(VI) b) Cu(II).

species of chromium detected by ESR analysis remain entrapped inside the beads and confirms the hypothesis formulated from EDX results that the reduced species of chromium could exchange with calcium ions of the beads. Escudero et al., 2017 also reported the absence of trivalent chromium in the final solutions in their study on Cr(VI) sorption onto natural sorbents encapsulated in calcium alginate. These authors suggested that reduced trivalent chromium remained inside the bead by retention of CA or microprecipitation on the natural sorbent.

3.3. Kinetics modelling

By using LAM model the coefficients D_e and α corresponding to Cr(VI) and Cu(II) sorption kinetics of the studied binary mixtures in both bench and pilot scale, have been determined and are the results presented in Tables 3 and 4, respectively.

As seen in Table 3, D_e and α of Cr(VI) for all initial Cr(VI) concentrations. Show the tendency to decrease with the increase of Cu(II) initial concentration, and to increase with the increase of Cr(VI) concentration. A similar trend was found to be followed by model parameters of Cr(VI) obtained by fitting pilot scale data (see Table 4). In the case of copper(II) model parameters, Table 3 shows that there is no clear trend of D_e of Cu(II) with the increase of Cr(VI) initial concentration, although a decreasing trend with the increase of initial copper(II) concentration is shown. In the same Table 3 it can be observed that the variation of α of Cu(II) with Cr(VI) initial concentration follows the opposite trend found for α of Cr(VI). The increase of a second metal ion initial concentration provokes a decrease of α of Cu(II) which increases as copper(II) initial concentration increases, showing again an opposite trend to the one observed for α of Cr(VI). Tendencies with respect to the increase of metal ions initial concentration for both D_e and α of Cu(II), obtained by fitting pilot plant data, could not be assessed (Table 4).

Data provided by the LAM model have been superimposed on the experimental data, as shown in Figs. 5–8 (solid lines): the model describes very well the kinetics in most cases.

The results presented in Tables 3 and 4 show that the model parameters D_e and α value vary as a function of the initial concentration of the metal ions in the mixture. One of the reasons for the dependence of these parameters with metal ions concentration is that the LAM was designed for modelling sorption of one component and so it does not take into account of interactions that exist between each other metal ions in the mixture. Therefore, in order to simulate the process outputs for non-studied initial concentrations, D_e and α must be estimated or experimentally determined.

As mentioned before D_e and α of Cr(VI) and Cu(II) obtained from bench data, showed a clear trends towards the variation of the second metal ion initial concentration in the mixture. With the aim of assessing the relationship between these two parameters and metal ions initial concentration, a quadratic empirical model was developed. Eqs. (11–14) correspond to the obtained fitting models:

$$D_{e,Cr} = k_{1,0} + k_{1,Cu}C_{Cu} + k_{1,Cr-Cu}C_{Cr}C_{Cu} \quad (11)$$

$$\alpha_{Cr} = k_{2,0} + k_{2,Cr}C_{Cr} + k_{2,Cr-Cu}C_{Cr}C_{Cu} \quad (12)$$

$$D_{e,Cu} = k_{3,0} + k_{3,Cu}C_{Cu} + k_{3,Cu-Cu}C_{Cu}^2 \quad (13)$$

$$\alpha_{Cu} = k_{4,0} + k_{4,Cu}C_{Cu} + k_{4,Cr-Cu}C_{Cr}C_{Cu} \quad (14)$$

The least squares method was used to obtain the coefficients ($k_{i,j}$ $i = 1, \ldots, 4$, j ∈{0, Cr, Cu, Cr − Cu, Cu − Cu}). This method is a multiple regression technique used to fit a mathematical model to a set of data generating the lowest residual.

The coefficients of the models and their significance level are shown in Table 5. As seen in the table, R^2 is in all the cases higher than 0.9 except in the case of D_e of copper.

The use of the developed empirical model is a new fast and easy approach to estimate D_e and α for any initial concentration of the metals in the binary mixture with the only restriction that the estimate concentrations have to be in the range of the studied concentrations. The

knowledge of these parameters allows simulating the corresponding sorption kinetics by using LAM model.

Simulated sorption data by LAM using the estimated D_e and α values by the empirical model of all experimentally bench studied binary mixtures, were also superimposed in Figs. 5 and 6 (dashed lines) showing a well fit of the experimental data.

In order to check that the empirical model provides a good estimation of the coefficients D_e and α obtained from the fit of bench experimental data with LAM, values of LAM coefficients have been plotted versus the estimated values by the empirical model (Fig. 9). The near zero intercept and the slope close to unity, confirm that the proposed model fits adequately the model parameters estimation.

4. Conclusions

This work demonstrates that a simplified diffusion model based on the Linear Adsorption Model is useful to describe the kinetics of a complex sorption system such as the simultaneous removal of Cr(VI) and Cu(II) by using exhausted coffee waste encapsulated in calcium alginate beads. The complexity of the global process lies in the different physical and chemical mechanisms taking place simultaneously that were identified and confirmed by spectroscopic analyses.

The major contribution of this paper is the development of the empirical model that combined with LAM model results in a useful, easy and time-saving new approach for describing metal ions kinetics of binary mixtures. The empirical model developed enables to estimate the LAM parameters (D_e and α) of metal ions binary mixtures provided that the initial concentration of the metal ions is included in the range of concentrations studied. The estimated values of the parameters introduced in LAM equation allow simulation of the corresponding binary mixture sorption kinetics.

This study constitutes a fast and easy approach to the modelling of sorption kinetics of complex systems in which different processes take place simultaneously.

Acknowledgements

This research was funded by the Spanish Ministry of Science and Innovation as part of the project CTM2015-68859-C2-1-R (MINECO-FEDER).

References

Aksu, Z., Egretli, G., Kutsal, T., 1998. A comparative study of copper (II) biosorption on Ca-alginate, agarose and immobilized *C. vulgaris* in a packed-bed column. Process Biochem. 33, 393–400.

Bai, R.S., Abraham, T.E., 2003. Studies on chromium (VI) adsorption-desorption using immobilized fungal biomass. Bioresour. Technol. 87, 17–26.

Cataldo, S., Cavallero, G., Gianguzza, A., Lazzara, g., Pettignano, A., Piazzese, D., Villaescusa, I., 2013. Kinetic and equilibrium study for cadmium and copper removal from aqeuous solutions by sorption onto mixed alginate/pectin gel beads. J. Environ. Chem. Eng. 1, 1252–1260.

Chen, J., Tendeyong, F., Yiacoumi, S., 1997. Equilibrium and kinetic studies of copper ion uptake by calcium alginate. Environ. Sci. Technol. 31, 1433–1439.

Crank, J., 1975. Mathematics of Diffusion. 2nd. edition. Clarendon Press, Oxford, London.

Escudero, C., Fiol, N., Villaescusa, I., 2006. Chromium sorption on grape stalks encapsulated in calcium alginate beads. Environ. Chem. Lett. 4, 239–242.

Escudero, C., Fiol, N., Villaescusa, I., Bollinger, J.-C., 2009. Arsenic removal by a waste metal (hydr)oxide entrapped into calcium alginate beads. J. Hazard. Mater. 164, 533–541.

Escudero, C., Fiol, N., Villaescusa, I., Bolllinger, J.-C., 2017. Effect of chromium speciation on its sorption mechanism onto grape stalks entrapped into alginate beads. Arab. J. Chem. 10, S1293–S1302.

Fiol, N., Poch, J., Villaescusa, I., 2005. Grape stalks wastes encapsulated in calcium alginate beads fro Cr(VI) removal from aqueous solution. Sep. Sci. Technol. 40, 1013–1028.

Fiol, N., Escudero, C., Poch, J., Villaescusa, I., 2006. Preliminary studies on Cr(VI) removal from aqueous soluton using grape stalk wastes encapsulated in calcium alginate beads in a packed bed up-flow column. React. Funct. Polym. 66, 795–807.

Fiol, N., Escudero, I., Villaescusa, I., 2008. Re-use of exhausted ground coffee waste for Cr(VI) sorption. Sep. Sci. Technol. 43, 582–596.

Liu, C., Fiol, N., Villaescusa, I., Poch, J., 2016. New approach in modelling Cr(VI) sorption onto biomass from metal binary mixtures solutions. Sci. Total Environ. 541, 101–108.

Garlaschelli, F., Alberti, G., Fiol, N., Villaescusa, I., 2017. Application of anodic stripping voltammetry to assess sorption performance of an industrial waste entrapped in alginate beads to remove as(V). Arab. J. Chem. 10, 1014–1021.

Haerifar, M., Azizian, S., 2013. An exponential kinetic model for adsorption at solid/solution interface. Chem. Eng. J. 215-216, 65–71.

Humar, M., Bokan, M., Amartey, S.A., Sentjurc, M., Kalan, P., Pohleven, F., 2004. Interaction of metals and prtons with algae 4. Ion exchange vs adsorption models and a reassessment of scatchard plots, ion-exchange rates an equilibrium compared with calcium alginate. Environ. Sci. Technol. 28, 1859–1866.

Ibañez, J., Umetsu, Y., 2002. Potential of protonated alginated beads for heavy metals uptake. Hydrometallurgy 64, 89–99.

Largitte, L., Pasquier, R., 2016. A review of kinetics adsorption models and their application to the adsorption of lead by an activated carbon. Chem. Eng. Res. Des. 109, 495–504.

Liu, Y., Liu, Y.-J., 2008. Biosorption isotherms, kinetics and thermodynamics. Sep. Purif. Technol. 61, 229–242.

Liu, C., Pujol, D., Olivella, M.À., de la Torre, F., Fiol, N., Poch, J., Villaescusa, I., 2015. The role of exhausted coffee compounds on metal ions sorption. Water Air Soil Pollut. 226, 289–299.

Ma, Z., Whitley, R.D., Wang, N.H.L., 1996. Pore and surface diffusion in multicomponent adsorption and liquid chromatography systems. AICHE J. 42 (5), 1244–1262.

Papageorgiou, S.K., Katsaros, F.K., Kouvelos, E.P., Nolan, J.W., Le Deit, H., Kanellopoulos, N.K., 2006. Heavy metal sorption by calcium alginate beads from *Laminaria digitata*. J. Hazard. Mater. B137, 1765–1772.

Placinski, W., Rudzinski, W., Placinska, A., 2009. Theoretical model of sorption kinetics including a surface reaction mechanism: a review. Adv. Colloid Interf. Sci. 152, 2–13.

Ponnusami, V., Rajan, K.S., Srivastava, S.N., 2010. Application of film-pore diffusion model for methylene blue adsorption onto plant leaf powders. Chem. Eng. J. 163, 236–242.

Pujol, D., Bartrolí, M., Fiol, N., Torre, F., Villaescusa, I., Poch, J., 2013. Modelling synergistic sorption of Cr(VI), Cu(II) and Ni(II) onto exhausted coffee wastes from binary mixtures Cr(VI)-Cu(II) and Cr(VI)-Ni(II). Chem. Eng. J. 230, 396–405.

Sag, Y., Aktay, Y., 2000. Mass transfer and equilibrium studies for the sorption of chromium ions onto chitin. Process Biochem. 36, 157–173.

Sag, Y., Nourbakhsh, M., Aksu, Z., Kutsal, T., 1995. Comparison of Ca-alginate and immobilized *Z. ramigera* as sorbent for copper (II) removal. Process Biochem. 30, 175–181.

Sillerová, H., Komàrek, M., Liu, C., Poch, J., Villaescusa, I., 2015. Biosorbent encapsulation in calcium alginate: effects of process variables on Cr(VI) removal from solutions. Int. J. Biol. Macromol. 80, 260–270.

Suksabye, P., Nakajima, A., Thiravetyan, P., Baba, Y., Nakbanpote, W., 2009. Mechanism of Cr(VI) adsorption by coir pith studied by ESR and asorption kinetic. J. Hazard. Mater. 141, 637–644.

Xu, Z., Cai, J., Pan, B., 2013. Mathematically modeling fixed-bed adsorption in aqueous systems. J. Zhejiang Univ. Sci. 14 (3), 155–176.